Geometric phases in a scattering process

H. D. Liu and X. X. Yi

Phys. Rev. A **84**, 022114 — Published 29 August 2011

DOI: 10.1103/PhysRevA.84.022114

Geometric phases in a scattering process

H. D. Liu and X. X. Yi
School of Physics and Optoelectronic Technology,
Dalian University of Technology, Dalian 116024, China

The study of geometric phase in quantum mechanics has so far be confined to discrete (or continuous) spectra and trace preserving evolutions. Consider only the transmission channel, a scattering process with internal degrees of freedom is neither a discrete spectrum problem nor a trace preserving process. We explore the geometric phase in a scattering process taking only the transmission process into account. We find that the geometric phase can be calculated by the some method as in an unitary evolution. The interference visibility depends on the transmission amplitude. The dependence of the geometric phase on the barrier strength and the spin-spin coupling constant is also presented and discussed.

PACS numbers: 03.65.Vf, 03.65.Ta, 11.15.-q

Berry's phase was originally introduced for bound states that an (discrete) eigenstate of the Hamiltonian would accumulate a geometric phase[1], when the evolution of the system is adiabatic. This Berry's phase provides us a very deep insight on the geometric structure of quantum mechanics and gives rise to various observable effects. The concept of the Berry phase has now become a central unifying concept in quantum mechanics, with applications in fields ranging from chemistry to condensed matter physics [2]. Recently the concept of Berry phase has been renewed and generalized for mixed states[3–6]. All these studies have been confined to discrete spectra.

For continuous spectrum, there are two things that can distinguish the geometric phase from bound states. (1) We always have non-Abelian gauge as a connection due to the degeneracy in this situation [7]; (2) The distortion of the Hamiltonian can not limited to a finite set of parameters, and hence we have to take into account the problem in an infinite-dimensional space. With these observations, the geometric phase factor has been considered for continuous spectra in [7], showing that the factor is exactly the scattering matrix. In Ref. [8], the scattering phase shift is defined in a way analogous to the adiabatic phase for bound states. This method works when reflection is negligible. By defining a virtual gap for the continuous spectrum through the notion of eigen-differential and using the differential projector operator, an explicit formula for a generalized geometrical phase is derived in terms of the eigenstates of the slowly time-dependent Hamiltonian[9]. These studies, in contrast with the case of discrete spectra, are all for systems with continuous spectra.

A scattering process with particles that have (pseudo) spin degrees of freedom is a typical phenomenon different from the aforementioned: The (discrete) internal spin degrees of freedom of the scattering particles inevitably couple to the (continuous) motional dynamics [10]. Hence such processes affect the state of the colliding spins according to quantum maps, instead of unitary operations. This makes the geometric phase acquired in such scattering processes distinct and interesting. Our main motivation in the present paper is to study the geometric phase in a scattering process with pseudo spin degrees of freedom. To tackle the problem, we focus on a gedanken setup consisting a quantum impurity, a mobile particle and two narrow potential barriers in each path of the double-slit, as shown in Fig. 1.

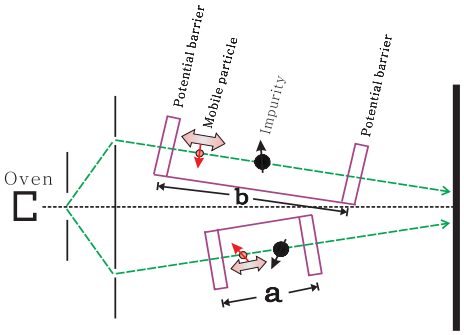

FIG. 1: (Color online) Illustration of a gedanken setup. A mobile particle can propagate along a wire in each path. A quantum impurity and two narrow potential barriers lie at $-\frac{a}{2}$ and $\frac{a}{2}$ in one path, and at $-\frac{b}{2}$ and $\frac{b}{2}$ in another. Once the mobile particle injected into one of the path, it undergoes multiple reflections between the barriers and impurity. Eventually, the mobile particle transmitted froward or reflected back. Consider only the transmission channel, this scattering process is not of trace-preserving. a (b) is the distance between the two barriers that we will refer to the width of structure in the text.

The mobile spin-1/2 particle e can propagate along the 1D path. A quantum impurity I, modeled as a spin-S scatterer, lies at $x = 0$, whereas two narrow potential barriers are located at $x = \pm x_0$ (the x-axis is along the path, $x_0 = a/2, b/2$ in Fig.1 for the two paths, respectively). The Hamiltonian for each path reads [11, 12] (we set $\hbar = 1$ throughout)

$$H = \frac{p^2}{2\mu} + J\delta(x)\vec{s}\cdot\vec{S} + G\left[\delta(x - x_0) + \delta(x + x_0)\right], \quad (1)$$

where μ and p are the effective mass and momentum operator of e, respectively, $\vec{s}$ and $\vec{S}$ stand respectively for the spin operators of e and I, J is a spin-spin coupling

constant and G is the potential-barrier strength. The above paradigmatic model naturally matches within a solid-state scenarios such as a 1D quantum wire [13] or single-wall carbon nanotube [14] with an embedded magnetic impurity or quantum dot[15]. Potential barriers are routinely implemented through applied gate voltages or heterojunctions.

Clearly, all of the scattering probability amplitudes are spin dependent due to the spin-spin contact potential $J\delta(x)\vec{s}\cdot\vec{S}$ in the Hamiltonian. As the overall spin space is D-dimensional ($D=[2\times(2S+1)]$), the effect of scattering is fully described by two $D\times D$ matrices whose generic elements respectively represent the amplitudes of reflection and transmission. These matrices can be derived by noting that the squared total spin of e and I as well as its projection along the z-axis are conserved. This entails that the dynamics within the singlet and triplet subspaces are decoupled. Consider only the transmission channel and assume that the injected state is

$$|\varphi_{in}\rangle = e^{ikx}|\uparrow\rangle\otimes|\phi_m\rangle, \tag{2}$$

the transmitted state takes,

$$|\varphi_{out}\rangle \;=\; e^{ikx}t_\uparrow|\uparrow\rangle\otimes|\phi_m\rangle + e^{ikx}t_\downarrow|\downarrow\rangle\otimes|\phi_{m+1}\rangle, \tag{3}$$

where $t_\uparrow$ and $t_\downarrow$ are the probability amplitudes for transmission with spin up and down, respectively. $|\phi_m\rangle$ are the eigenstates of S_z (the z-component of $\vec{S}$), i.e., $S_z|\phi_m\rangle = m|\phi_m\rangle$, and $k=\sqrt{2\mu E}$ with $E>0$ being the energy of the injected particle. $|\uparrow\rangle$ and $|\downarrow\rangle$ denote the eigenstates of s_z for the mobile particle. The dependence of $t_\uparrow$ and $t_\downarrow$ on G, J and x_0 can be established by

$$t_\uparrow = t_\uparrow(x_0) = \{1+i[\chi-(m+1)j']\}/\Delta, \tag{4}$$

$$t_\downarrow = t_\downarrow(x_0) = -ij'F/\Delta, \tag{5}$$

where $j'=|W|^2j/(2\kappa)$, $\Delta=(1+i\chi)[1+i(\chi-j')]+S(S+1)j'^2$ and $F=[(S-m)(S+m+1)]^{1/2}$, with $W=1+g\sin(2\kappa\alpha)+i2g\sin^2(\kappa\alpha)$, and $\chi=2g[g\sin(2\kappa\alpha)+\cos(2\kappa\alpha)]$. To simplify the problem, the following dimensionless quantities were defined: $j=J/(2a_B\varepsilon)$, $\kappa=ka_B=\sqrt{E/\varepsilon}$, $g=G/(2ka_B\varepsilon)$, and $\alpha=x_0/a_B$. Here a_B is the Bohr radius, $\varepsilon=1/(2\mu)a_B^2$ and $2x_0$ is the distance between the two potential barriers, which we will call the width of structure in this paper.

Consider a situation where the width of the structure on each path is different but the spin-spin coupling constant and the barrier strength on both paths are the same. We have interests in the phase difference between the mobile particles transmitted through different paths. This phase difference consists of a dynamical phase and a geometrical part. Our task here is to extract the geometric phase from the total part $\Gamma=\arg\langle\varphi_{out}(a)|\varphi_{out}(b)\rangle$. This can be done by either parallel transport of the state or canceling the dynamical phase. The parallel transport condition in this case is $\Im\langle\varphi_{out}(x_0)|\frac{\partial}{\partial x_0}|\varphi_{out}(x_0)\rangle=0$, leading to the geometric phase in the scattering process,

$$\gamma_s = \arg\left(\langle\varphi_{out}(a)|\varphi_{out}(b)\rangle e^{-i\Im(\int_a^b \frac{\langle\varphi_{out}(x_0)|\frac{\partial}{\partial x_0}|\varphi_{out}(x_0)\rangle}{\langle\varphi_{out}(x_0)|\varphi_{out}(x_0)\rangle}dx_0)}\right), \tag{6}$$

where $\Im(...)$ denotes the imaginary part of $(...)$. We now prove that γ_s defined in Eq. (6) is geometric, i.e., it only depends on the trajectory traced out by $|\varphi_{out}(x_0)\rangle$. Define a quantum map by

$$M(b,a) = |\varphi_{out}(b)\rangle\langle\varphi_{out}(a)|, \tag{7}$$

the total phase Γ acquired in the scattering process can be written as $\Gamma=\arg\langle\varphi_{out}(a)|M(b,a)|\varphi_{out}(a)\rangle$. Notice that

$$\bar{M}(b,a) = M(b,a)e^{i\beta(b,a)}|\varphi_{out}(a)\rangle\langle\varphi_{out}(a)| \tag{8}$$

with real parameters $\beta(b,a)$ and $\beta(a,a)=0$ gives the same state $|\bar{\varphi}_{out}(b)\rangle$, since $|\bar{\varphi}_{out}(b)\rangle = e^{i\beta(b,a)}|\varphi_{out}(b)\rangle$ differs from $|\varphi_{out}(b)\rangle$ only in an overall phase $\beta(b,a)$. Parallel transport condition $\Im\langle\varphi_{out}(x_0)|\frac{\partial}{\partial x_0}|\varphi_{out}(x_0)\rangle=0$ leads to

$$\Im\langle\varphi_{out}(0)|\bar{M}^\dagger(x_0,0)\frac{\partial}{\partial x_0}\bar{M}(x_0,0)|\varphi_{out}(0)\rangle = 0. \tag{9}$$

Substituting Eq. (8) into Eq.(9), we have

$$\beta(b,a) = -\int_a^b \frac{\Im\langle\varphi_{out}(x_0)|\frac{\partial}{\partial x_0}|\varphi_{out}(x_0)\rangle}{\langle\varphi_{out}(x_0)|\varphi_{out}(x_0)\rangle}dx_0. \tag{10}$$

This completes the proof. For our scattering problem, simple algebra yields,

$$\gamma_s = \arg\left[(t^*_\uparrow(a)t_\uparrow(b) + t^*_\downarrow(a)t_\downarrow(b))e^{-i\int_a^b \frac{1}{|t_\uparrow|^2+|t_\downarrow|^2}(|t_\uparrow|^2\frac{\partial\phi_\uparrow}{\partial x_0}+|t_\downarrow|^2\frac{\partial\phi_\downarrow}{\partial x_0})dx_0}\right]. \quad (11)$$

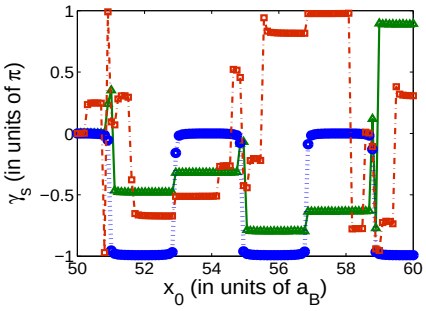

FIG. 2: (Color online) The geometric phase γ_s versus one width of structure, while another width of structure is fixed to $50a_B$ (say, for example, the width of the lower structure is $50a_B$). Parameters chosen are: $J \to 0$ (10^{-6}) for blue circle; $J = 11$ for red square and $J = 50$ for green triangle. The other parameters: $k = 0.8$, $a_B = 1$, $G = 10$, $m = -\frac{1}{2}$, $\varepsilon = 1$, $S = \frac{1}{2}$.

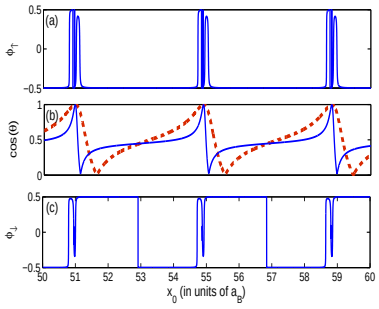

FIG. 3: (Color online) Angle $\phi_\uparrow$ and $\phi_\downarrow$ (in units of π), and $\cos(\theta)$ as a function of the width of structure. $J = 50$ was taken for the plot. The red dashed line in (b) is for $J = 11$. The other parameters chosen are the same as in Fig.2. $\cos\theta$ was defined by $\cos\theta \equiv \frac{|t_\uparrow|}{\sqrt{|t_\uparrow|^2+|t_\downarrow|^2}}$.

Here, $\phi_{\uparrow(\downarrow)}$ was defined by

$$\tan\phi_{\uparrow(\downarrow)} \equiv \frac{t^I_{\uparrow(\downarrow)}}{t^R_{\uparrow(\downarrow)}}.$$

$t^I_{\uparrow(\downarrow)}$ and $t^R_{\uparrow(\downarrow)}$ denote the imaginary and real part of $t_{\uparrow(\downarrow)}$, respectively. The geometric phase given in Eq.(11) represents the difference in geometric phase for the mobile particle transmitted through the two paths. We will show later that it coincides with the geometric phase acquired in an unitary evolution treating the width as time t.

We have performed numerical calculations for Eq.(11), results are presented in Fig.2– Fig.7. For simplicity,

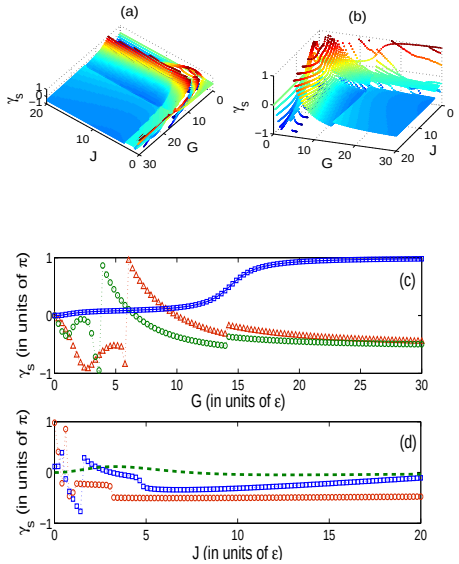

FIG. 4: (Color online) γ_s (in units of π) as a function of the barrier strength G (in units of ε) and spin-spin coupling constant J (in units of ε). (a) and (b) are same, but show the dependence from different angle. In (c), different lines are for different J, $J \to 0$ for blue square line, $J = 11$ for green circle, and $J = 30$ for red triangle. In (d), $G = 0.1$ for green dashed line, $G = 9$ for blue square line, and $G = 30$ for red circle line. $k = 1.6$ (in units of ε) is chosen for this plot. For other parameters, see Fig. 2. The widths of the two structures are $50a_B$ and $60a_B$, respectively.

$S = \frac{1}{2}$ was specified without loss of generality. Fig.2 shows the dependence of the geometric phase γ_s on the width difference (i.e., one width of the structure, say a, is fixed to $50a_B$, while another changes from $50a_B$ to $60a_B$ in Fig.1) for different spin-spin coupling constant. We find that the mobile particle acquires either 0 or $-\pi$ geometric phase when $J \to 0$ ($J = 10^{-6}$ was taken for the plot). Sharp changes in the geometric phase happen periodically, regardless of what value J takes. Moreover we find that the geometric phase change its value only at the points where $t_\uparrow$ and $t_\downarrow$ change abruptly, as shown in Fig.3. We observe three resonances from Fig.3, corresponding to $\cos\theta = 1$. As the spin-spin coupling constant J approaches the barrier strength G, the resonance region becomes wide (see the red-dashed line in Fig.3(b)). Further examination shows that these points coincide with the condition for resonant widths given by $\cot(2\kappa\alpha) = -g$ (i.e., $|t_\uparrow| = 1$). Besides, from Eqs (4) and (5) we find that the width of structure x_0 enters $t_\uparrow$ and $t_\downarrow$ only through $\cos(2\kappa\alpha)$ and $\sin(2\kappa\alpha)$, this determines

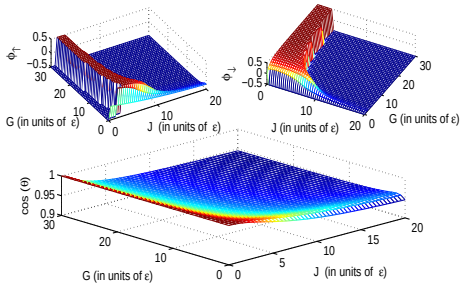

FIG. 5: (Color online) Angle $\phi_\uparrow$ and $\phi_\downarrow$ (in units of π), and $\cos(\theta)$ as a function of the barrier strength G and spin-spin coupling constant J. In this plot $k = 1.6$, the width of structure is $60a_B$. The other parameters chosen are the same as Fig.2. Note that $\phi_\downarrow = 0$ when $J \to 0$.

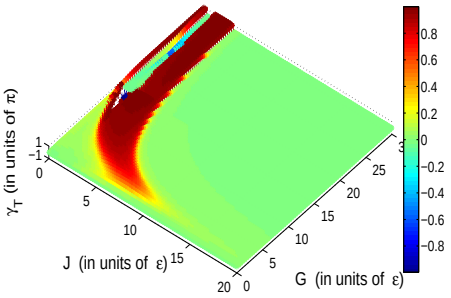

FIG. 6: (Color online) γ_T as a function of the barrier strength G and spin-spin coupling constant J. In this plot $k = 1.6$. For other parameters, see Fig. 2. The widths of the two structures are $50a_B$ and $60a_B$, respectively.

the period of these sharp changes. The spin-spin coupling smooth the sharpness of the changes, this is due to the broadening of the width resonance (see Fig.3(b), red dashed line). The geometric phase keeps constant except at the sharp change points, this results from the fact that $\phi_\uparrow$, $\phi_\downarrow$ and $\cos\theta$ are (almost) constant at the off-resonant points (see Fig. 3). The physics behind these observations can be understood as follows. At the resonant points where $\cos\theta$ changes from 1 to 0 suddenly, spin flips happens, and at the point of $\cos\theta = 1/2$, $t_\downarrow$ gains a π phase, due to the change in the width of structure.

The dependence of the geometric phase on the spin-spin coupling is shown in Fig.4. Note that $\gamma_s = 0$ when $G \to 0$, see Fig.4(c). This can be understood by examining the limit of $g \to 0$. In this limit, $t_\uparrow \simeq (1-i0.5j')/(1-ij'+1.5j'^2)$, $t_\downarrow \simeq (-ij')/(1-ij'+1.5j'^2)$. Clearly, both $t_\uparrow$ and $t_\downarrow$ do not depend on the width of the structure, thus the system can not acquire a geometric phase as $G \to 0$. This is, however, not the case for $J \to 0$ as Fig.4 (d) shows. In the limit of $J \to 0$, $t_\uparrow \simeq \frac{1}{1+i\chi}$, and $t_\downarrow \simeq 0$. But $\partial\phi_\downarrow/\partial t$ may be very large. Because χ depends on the width, the geometric phase in this case is not always zero. Note that by Eq.(5), $J = 0, t_\downarrow = 0$. In the strong spin-spin coupling ($J \to \infty$) and large barrier strength limit ($g \to \infty$), we have $\phi_\uparrow = \phi_\downarrow$ and $t_\downarrow = 2t_\uparrow$, this leads to the geometric phase,

$$\gamma_s = \arg\left(t_\uparrow^*(a)t_\uparrow(b)e^{-i2(\phi_\uparrow(b)-\phi_\uparrow(a))}\right). \qquad (12)$$

Therefore for fixed a and b, the geometric phase γ_s tends to constants with $J \to \infty$ and $G \to \infty$ (see Fig. 4(a) and (b)). This results from the dependence of $\phi_\uparrow$, $\phi_\downarrow$ and $\cos\theta$ on J and G. In fact, for a width of structure $x_0 = 60a_B$ and injected energy $k = 1.6\varepsilon$, the spin up with probability $|t_\uparrow|^2$ dominates the transmission channel (see Fig.5), as J and G tends to ∞, both $\phi_\uparrow$ and $\phi_\downarrow$ approach $-\frac{\pi}{2}$ due to $t^I_{\uparrow,\downarrow} \gg t^R_{\uparrow,\downarrow}$.

Define $\gamma_T = \arg\left(t_\uparrow^*(a)t_\uparrow(b) + t_\downarrow^*(a)t_\downarrow(b)\right)$ as the total phase acquired in the scattering process, and

$$\gamma_d = \int_a^b \frac{1}{|t_\uparrow|^2 + |t_\downarrow|^2}(|t_\uparrow|^2\frac{\partial\phi_\uparrow}{\partial x_0} + |t_\downarrow|^2\frac{\partial\phi_\downarrow}{\partial x_0})dx_0$$

as the dynamical phase, we have from Eq. (11) that the geometric phase is $\gamma_s = \gamma_T - \gamma_d$. The total phase as a function of the spin-spin coupling constant and the barrier strength is given in Fig.6. Clearly, as G and J tend to ∞, γ_T approaches zero, suggesting that for large G and J, the width difference has no contribution to the geometric phase, this is confirmed by Fig. 5. Mathematically, both $t_\downarrow$ and $t_\uparrow$ take imaginary values when G and J approach ∞, the total phase γ_T is then zero.

In Ref. [7], the authors consider the geometric phase factor in quantum mechanics for the case of continuous spectrum. At first glance, this paper presents nothing for continuous degrees of freedom. Now we show that, to a sense, the present study really sheds light on this issue. As aforementioned, the transmission rate of injected spin depends on the energy of the spin, and the wavefunction in the transmission channel is an eigenstate of the kinetic Hamiltonian $p^2/2m$, with the corresponding eigenenergy $k^2/2m$. k may take continuous value, implying that the spectrum is continuous. The initial energy (state) of the mobile spin affects the geometric phase acquired in the scattering process. The dependence of the geometric phase γ_s on k of the injected spin is presented in Fig.7. We find that for $G \to 0$, the spin acquires null geometric phase as k tends to ∞, whereas with $J \to 0$, the geometric phase approaches 0 or $\pm\pi$ when $k \to \infty$. This confirms the discussion made below Fig.4. These results show that the initially continuous/motional state of the injected spin can affect the geometric phase in the scattering process. In this sense, the present study shed light on the issue of geometric phase in continuous spectrum problem.

To explore the dependence of the geometric phase on the initial state of the localized spin, we plot γ_s as a function of m in Fig.8, where S, J and G are fixed for each line. We find from Eq.(5) that $t_\downarrow = 0$ when $m = S$,

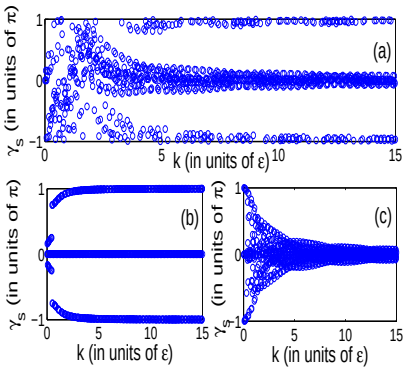

FIG. 7: (Color online)γ_s as a function of k of the injected particle. (a), (b) and (c) are different for J and G. (a) $J = 2.2$ and $G = 1.8$; (b) $J \to 0$ and $G = 1.8$; (c) $G \to 0$ and $J = 2.2$. The widths of the two structures are fixed to $50a_B$ and $60a_B$, respectively.

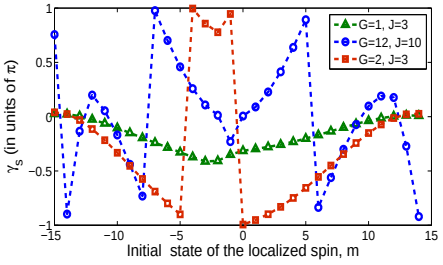

FIG. 8: (Color online)γ_s as a function of the initial state of the localized spin characterized by m. In this plot, $k = 1.6$ and $S = 15$. Note that when $m = S$, the geometric phase is zero (not shown in the figure) due to $t_\downarrow = 0$. The widths of the two pathes are $50a_B$ and $60a_B$, respectively.

leading to a null geometric phase in this case. In addition, when J and G are small with respect to S, $j' \ll S(S+1)$, if F defined in Eq.(5) is much smaller than $|\Delta|$, $|t_\downarrow|$ can be ignored, then the spin acquires no geometric phase. This is exactly the case when $|m| \simeq S$, see square red line and triangle green line in Fig. 8. A common feature in Fig. 8 is that the line is not symmetric about $m = 0$, this can be interpreted as different contributions of $-m$ and m to Eqs (4) and (5).

It is interesting to note that $m = 0$ and $m = -1$ give the same F defined in Eq.(5), then $t_\downarrow(m = 0) = t_\downarrow(m = -1)$. As spin-spin coupling becomes stronger and the barrier strength tends to larger, the changes of the geometric phase with m become more evident. We interpret this feature as the sensitivity of the geometric phase to the state to the localized spin, i.e., the larger the G and J are, the more sensitive of γ_s to m.

Now we are in a position to explore, in terms of geometric phase, what is the difference between the normalized and non-normalized transmitted state. To this end, we define

$$\cos\theta \equiv \frac{|t_\uparrow|}{\sqrt{|t_\uparrow|^2 + |t_\downarrow|^2}},$$

the transmitted state can be rewritten as,

$$|\varphi_{out}\rangle = \cos\theta e^{i\phi_\uparrow}|\uparrow\rangle\otimes|\phi_m\rangle + \sin\theta e^{i\phi_\downarrow}|\downarrow\rangle\otimes|\phi_{m+1}\rangle. \quad (13)$$

We point out that by the conservation of current probability, we have $|t_\uparrow|^2 + |t_\downarrow|^2 = 1 - |r_\uparrow|^2 - |r_\downarrow|^2 \le 1$. Here we consider only the transmission channel, and the transmitted state has been normalized, this would only affect the visibility of the interference fringes but not shift the patterns. By the definition of geometric phase for an unitary evolution, we have

$$\gamma_s' = \arg\left((\cos\theta(b)\cos\theta(a)e^{i(\phi_\uparrow(b)-\phi_\uparrow(a))} + \sin\theta(b)\sin\theta(a)e^{i(\phi_\downarrow(b)-\phi_\downarrow(a))})e^{-i\int_a^b(\dot\phi_\uparrow\cos^2\theta + \dot\phi_\downarrow\sin^2\theta)dx_0}\right), \quad (14)$$

where $\dot\phi_\uparrow \equiv \frac{\partial\phi_\uparrow}{\partial x_0}$, $\dot\phi_\downarrow \equiv \frac{\partial\phi_\downarrow}{\partial x_0}$. Recall that the real part of $\langle\varphi_{out}(a)|\varphi_{out}(b)\rangle$ represents the visibility of the interference pattern, we conclude that the geometric phase for the non-normalized and normalized transmitted state are the same, namely, $\gamma_s' = \gamma_s$. **This observation connects the conventional interpretation of the geometric phase to the geometric phase acquired in this scattering process. I.e., the geometric phase acquired in a scattering process can be understood as the solid angle on the Bloch sphere, characterized by θ and ϕ.** One may concern about the observation of the geometric phase, in particular worry about the separation of the geometric phase from the total phase. In general, by varying the width difference $(b - a)$, it is possible to make the dynamical part of phase the same for the two beams.

In conclusion, the geometric phase in a scattering process is studied in this paper. Consider only the transmission channel, the scattering process is neither a trace-preserving dynamics nor a discrete spectrum problem. Instead it concerns the coupling between the internal degrees of freedom and the motional dynamics, and it can be described by quantum map to replace the unitary evolution. We have defined and calculated the geomet-

ric phase in such a process and show the dependence of the geometric phase on the spin-spin coupling constant and the barrier strength. **We find that the geometric phase changes sharply at the points of resonance scattering, where the system (the moving particle)** *jump* **from one point on the Bloch sphere to the others. At the points far from resonance scattering, the geometric phase tends to a constant (0, or π)when one of the parameters (e.g., the barrier strength G, the spin-spin coupling constant J, and the momentum k) tends to infinity, while the others keep constants.** Possible observation of the geometric phase is suggested and discussed.

This work is supported by NSF of China under grant Nos 61078011 and 10935010.

[1] M. V. Berry, Proc. R. Soc. London A 392, 45(1984).

[2] Geometric phase in physics, Edited by A. Shapere and F. Wilczek (World Scientific, Singapore, 1989).

[3] E. Sjöqvist, A.K. Pati, A. Ekert, J.S. Anandan, M. Ericsson, D.K.L. Oi, and V. Vedral, Phys. Rev. Lett. **85**, 2845 (2000).

[4] D. M. Tong, E. Sjöqvist, L. C. Kwek, C. H. Oh, Phys. Rev. Lett. 93, 080405 (2004).

[5] X.X. Yi, L.C. Wang, and T.Y. Zheng, Phys. Rev. Lett. 92, 150406 (2004); X. X. Yi, and E. Sjöqvist, Phys. Rev. A 70, 042104 (2004); L. C. Wang, H. T. Cui, and X. X. Yi, Phys. Rev. A 70, 052106 (2004).

[6] F. M. Cucchietti, J.-F. Zhang, F. C. Lombardo, P. I. Villar, and R. Laflamme, Phys. Rev. Lett. **105**, 240406 (2010).

[7] R. G. Newton, Phys. Rev. Lett **72**, 954 (1994).

[8] G. Ghosh, Phys. Lett. A **210**, 40 (1996).

[9] M. Maamache and Y. Saadi, Phys. Rev. Lett. **101**, 150407 (2008).

[10] Z. Tang and D. Finkelstein, Phys. Rev. Lett. **74**, 3134 (1995).

[11] O. L. T. de Menezes and J. S. Helman, Am. J. Phys. **53**, 1100 (1985).

[12] G. Cordourier-Maruri, F. Ciccarello, Y. Omar, M. Zarcone, R. de Coss, and S. Bose, arXiv:1008.2370.

[13] J. H. Davies *The Physics of Low-Dimensional Semiconductors: an Introduction* (Cambridge University Press, Cambridge, U.K., 1998)

[14] S. J. Tans, M. H. Devoret, H. Dai H, A. Thess, R. E. Smalley, L. J. Geerligs , and C. Dekker, Nature **386**, 474 (1997).

[15] F. Ciccarello *et al.*, New J. Phys. **8**, 214 (2006); J. Phys. A: Math. Theor. **40**, 7993 (2007); F. Ciccarello, G. M. Palma, and M. Zarcone, Phys. Rev. B **75**, 205415 (2007); F. Ciccarello, M. Paternostro, G. M. Palma and M. Zarcone, Phys. Rev. B **80**, 165313 (2009).